Unsteady Interactions among Multiple Ships with Free-Surface Effects

Zhi-Ming Yuan[1] and Ronald W. Yeung[2,*]

[1]University of Strathclyde, UK
[2]University of California at Berkeley, USA
*Correspondence author, E-mail: rwyeung@berkeley.edu, Tel.: +1 (510) 642-8347

ABSTRACT

Ships often have to pass each other in proximity in harbor area and waterways in dense shipping traffic environment. Hydrodynamic interaction occurs when a ship is overtaking (or being overtaken) or encountering other ships. Such an interactive effect could be magnified in confined waterways, *e.g.* shallow and narrow rivers. Since Yeung (1978) published his initial work on ship-interaction in shallow water, progress on unsteady interaction among multiple ships has been slow though steady over the following decades. With some exceptions, nearly all the published studies on ship-to-ship problem neglected free-surface effects, and a rigid wall condition has often been applied on the water surface as the boundary condition. When the speed of the ships is low, this assumption is reasonably accurate, as the hydrodynamic interaction is mainly induced by near-field disturbances. However, in many maneuvering operations, the encountering or overtaking speeds are actually moderately high (Froude number F_n>*0.2,* where $F_n \equiv U/\sqrt{gL}$, U is ship speed, g the gravitational acceleration and L the ship length), especially when the lateral separation between ships is the order of ship length. Here, the far-field effects arising from ship waves can be important. The hydrodynamic interaction model must take into account of the surface-wave effects.

Classical potential-flow formulation is only able to deal with the boundary value problem (BVP) when there is only one speed involved in the free-surface boundary condition. For multiple ships travelling with different speeds, it is not possible to express the free-surface boundary condition by a single velocity potential. Instead, a superposition method can be applied to account for the velocity field induced by each vessel with its own and unique speed. The main objective of the present paper is to propose a rational superposition method to handle the unsteady free-surface boundary condition containing two or more speed terms, and validate its feasibility in predicting the hydrodynamic behaviour of the ships during overtaking or encountering operations. The solution methodology used in the present paper is a three-dimensional boundary-element method (BEM) based on a Rankine-type (infinite-space) source function, initiated introduced in Bai & Yeung (1974). The numerical simulations are conducted by using an in-house developed multi-body hydrodynamic interaction program "MHydro". Waves generated and forces (or moments) are calculated when ships are encountering or passing each other. Published model-test results are used to validate our calculations and very good agreement has been observed. The numerical results show that free-surface effects need to be taken into account for $F_n > 0.2$.

INTRODUCTION

Ship-to-ship interaction problem is a classical hydrodynamics problem which has been widely studied over the last few decades. No matter which kind of methods is used, at least one or more of the following important assumptions are often adopted to simplify the problem:

1) The fluid is ideal and viscous effects are neglected.
2) The speed is low and free-surface deformation effects are negligible (rigid-wall free-surface is applicable).
3) The ships are slender.
4) The shedding of cross-flow vorticity is either ignored, or idealized in a manner similar to thin-wing theory.

During1960s-1990s, the slender-body theory has been widely popular to predict the hydrodynamic interaction between multiple ships (Collatz, 1963; Tuck, 1966; Tuck and Newman, 1974; Dand, 1975; Yeung, 1975, 1978; Kijima and Yasukawa, 1985; Varyani et al., 1998). All of the assumptions mentioned above were adopted in the cited studies.

These assumptions significantly simplified the mathematical model and led to high-efficiency numerical calculations. For conventional ships travelling at relatively low Froude numbers, the numerical calculations based on strip theory showed a fairly good prediction of the sway force and yaw moment on ships during overtaking or meeting operations. To account for the three-dimensional effects and remove the geometrical idealization described in Assumption 3, Korsmeyer *et al*. (1993) adopted a three-dimensional panel method, which is applicable to any number of arbitrarily shaped bodies in arbitrary motions. Pinkster (2004) extended Korsmeyer's method with implementation of a model to account for the free-surface effects partially. His model was restricted to simulating the effect of a passing ship on a moored ship. Only the low frequency seiche or solitary waves were taken into account, while the more important far-field waves or so-called Kelvin waves were neglected. Therefore, his conclusions on free-surface effects could not cover the general ship-to-ship operations. More recently, three-dimensional panel method has been more commonly used (Söding and Conrad, 2005; Xiang and Faltinsen, 2010; Zhou et al., 2012; Xu et al., 2016). which began to investigate the effects of unsteady free-surface waves on the interaction forces. The general conclusion drawn from these studies is that the potential-flow solver could provide a good prediction of interaction forces on ships travelling at relatively low Froude numbers. Within this framework there exist potential-flow codes such as Pinkster (2013) or Fenfach et al. (2011) that handle ships moving over sloppy bottom or harbour entrances. Benefitted from improving CFD (Computational Fluid Dynamics) technology, viscous effects on ship-to-ship problem have been investigated using various turbulence models (Zou and Larsson, 2013b; Jin et al., 2016; Sian et al., 2016, Meng and Wan, 2016). The free-surface effects are either neglected (Zou and Larsson, 2013b) or treated simply as a steady problem (Jin et al., 2016; Sian et al., 2016). In these Navier-Stokes model, few efforts were made to investigate the long-time unsteady free-surface waves produced by two or more ships moving with different speeds. The demand in computational power when more than one ship is passing can be the bottleneck if real-time applications should be needed.

The unsteady free-surface wave effect is not essential when the encountering or overtaking speed is low. However, in the waterways with dense shipping traffic, the encountering or overtaking speed is not always low. As shown in **Figure 1**, the far-field waves generated by the encountering ships are obviously observed. A strong unsteady interaction between ships can be excited by the unsteady free-surface waves. Furthermore, the existence of the river banks traps the waves from propagating to either sides, which makes the interference problem more complicated. Therefore, the rigid free-surface condition is not capable of predicting the hydrodynamic interactions induced by far-field waves. A new approach is proposed to deal with the free-surface boundary condition.

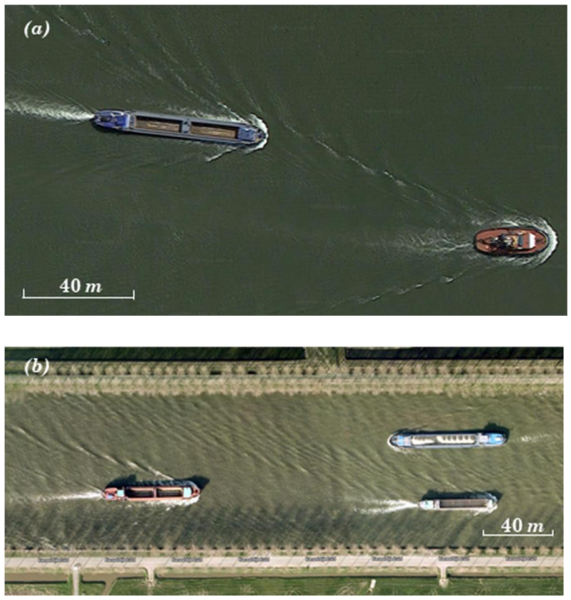

Figure 1: A satellite image taken from the Google Earth database showing the wave interference effect in confined waterways. (a) Two ships in overtaking operation in Nieuwe Maas, The Netherlands[1]; (b) Encountering ships in Amsterdam–Rhine Canal, The Netherlands[2].

The main challenge of imposing a non-rigid free-surface condition arises from the speed term in the body boundary condition (See Eq. (16) later). For multiple ships travelling with various speeds, it is not possible to express the free-surface boundary condition by a single velocity potential (unless one uses a earth-fixed coordinate system as in Yeung (1975)). A superposition method, however, can be applied to account for the velocity potentials induced by each vessel with its own, unique speed. In order to account for the different speeds appearing in free-surface boundary condition, Yuan et al. (2015) proposed an uncoupled method based on the superposition principle. Therein, the speed difference of two ships was assumed to be small. Thus, the free-

[1] https://www.google.co.uk/maps/@51.9005594,4.3688259,390m/data=!3m1!1e3?authuser=1

[2] https://www.google.co.uk/maps/@52.0098121,5.1658702,427m/data=!3m1!1e3?authuser=1

surface condition could be treated (arguably) as steady-state problem. This method is not applicable to predict the interaction forces when ships' speeds are not the same, or when two ships are moving towards each other. In these cases, the unsteady effect becomes essential and the time-dependent terms must be taken into account. In the present study, we will extend Yuan's method to the time domain and discuss the importance of free-surface effects on multi-ship problem.

THE BOUNDARY-VALUE PROBLEM

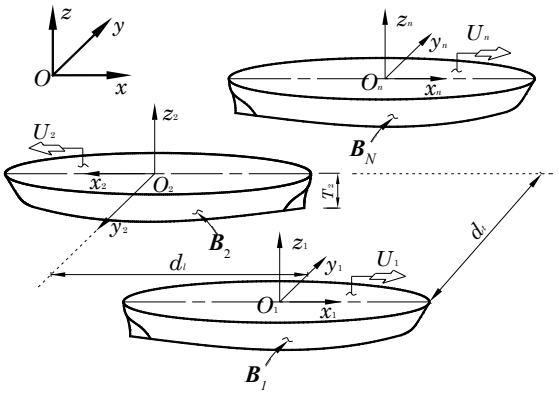

Figure 2: Coordinate systems.

Consider N ships moving at speeds U_j (j = 1, 2, ..., N) with respect to a space-fixed reference frame $\mathbf{x} = (x, y, z)$ in an inviscid fluid of depth h as shown in Figure 2. A right-handed Cartesian coordinate system $\mathbf{x_j} = (x_j, y_j, z_j)$ (j = 1, 2, ..., N) is fixed to each ship with its positive x_j-axis pointing towards the bow, positive z-axis pointing upwards and z_j = 0 being the undisturbed free-surface. Let Φ ($\mathbf{x}$, t) be the velocity potential describing the disturbances generated by the forward motion of the ships and ζ (x, y, t) be the free-surface elevation. In the fluid domain, the total velocity potential Φ satisfies the Laplace equation

$$\nabla^2 \Phi(\mathbf{x}, t) = 0 \tag{1}$$

The fluid pressure, $p(\mathbf{x}, t)$, is given by Euler's integral:

$$p(\mathbf{x}, t) = -\rho\left(\frac{\partial \Phi}{\partial t} + \frac{1}{2}\nabla\Phi \cdot \nabla\Phi + gz\right) + p_0 \tag{2}$$

where ρ is the fluid density, p_0 is the atmospheric pressure, which is used as a reference pressure and assumed to be constant. Assuming there is no overturning and breaking waves on the free-surface, we can use this Eulerian description of the flow to describe the free-surface motion. The free-surface elevation is given by $z = \zeta(x, y, t)$. A fluid particle on the free-surface is assumed to stay on the free-surface, which leads to the following kinematic free-surface boundary condition:

$$\frac{D}{Dt}(\zeta - z) = 0 \text{, on } z = \zeta \tag{3}$$

The material derivative in Eq. (3) is given by:

$$\frac{D}{Dt} = \frac{\partial}{\partial t} + \nabla\Phi \cdot \nabla \tag{4}$$

The dynamic free-surface condition is that the fluid pressure equals the constant atmospheric pressure p_0 on the free-surface, with the position of the free-surface being unknown. According to the Euler's integral Eq. (2), the dynamic free-surface boundary condition can be written as:

$$\frac{\partial \Phi}{\partial t} + \frac{1}{2}\nabla\Phi \cdot \nabla\Phi + gz = 0 \text{ , on } z = \zeta \tag{5}$$

By applying Taylor series expanded about z = 0 and only keeping the linear terms, the dynamic and kinetic free-surface conditions can be linearized as

$$\frac{\partial \zeta}{\partial t} - \frac{\partial \Phi}{\partial z} = 0 \text{, on } z = 0 \tag{6}$$

$$\frac{\partial \Phi}{\partial t} + g\zeta = 0 \text{, on } z = 0 \tag{7}$$

Combining Eq. (6) and (7), we obtain the free-surface boundary condition:

$$\frac{\partial^2 \Phi}{\partial t^2} + g\frac{\partial \Phi}{\partial z} = 0 \text{, on } z = 0 \tag{8}$$

It should be noted the free-surface elevation ζ can be found from Eq. (7) when the velocity potential Φ is known. On the wetted hull surface, the no-flux boundary conditions are used, and the following 'exact' boundary condition can be formulated:

$$\frac{\partial \Phi}{\partial n} = U_j \left(n_x\right)_j \text{ on } B_j, \text{ where } j = 1, 2, \ldots, N \tag{9}$$

where $\partial/\partial n$ is the derivative along the normal vector $\mathbf{n} = (n_x, n_y, n_z)$ on the hull surface. We choose the normal vector to point outwards of the fluid domain.

Assuming the disturbance of the fluid is small, we represent the total velocity potential produced by the presence of all ships in the fluid domain in a space-

fixed frame to satisfy the following superposition principle:

$$\Phi(\mathbf{x},t)=\sum_{j=1}^{N}\Phi_j(\mathbf{x},t)\,,\ j = 1, 2, \ldots, N \tag{10}$$

where $\Phi_j(\mathbf{x}, t)$ is the velocity potential produced by the presence of ship j moving with U_j, while the remaining ships are momentarily stationary in this frame. For the linear problem, the body-fixed coordinate system $\mathbf{x_j} = (x_j, y_j, z_j)$ ($j = 1, 2, \ldots, N$) is used to solve the BVP for N vessels in concurrent motion. The relation between the body- and space-fixed coordinate system is straightforward, viz.

$$x_j = x - U_j t\,,\ j = 1, 2, \ldots, N \tag{11}$$

Let $\phi_j(\mathbf{x_j}, t)$ represents $\Phi_j(\mathbf{x}, t)$ in the body-fixed coordinate system, the following relation can be obtained

$$\frac{d\Phi_j}{dt}=\left(\frac{\partial}{\partial t}-U_j\frac{\partial}{\partial x_j}\right)\phi_j \tag{12}$$

The velocity potential ϕ_j satisfies the Laplace equation and body 'exact' boundary condition:

$$\nabla^2\phi_j(\mathbf{x_j},t)=0\,,\ j = 1, 2, \ldots, N \tag{13}$$

$$\frac{\partial\phi_j}{\partial n}=\delta_{ij}U_j\left(n_x\right)_j\,,\ \text{on } B_i,\ i,j = 1, 2, \ldots, N \tag{14}$$

The Kronecker delta δ_{ij} is defined by:

$$\delta_{ij}=\begin{cases}1 & i=j\\ 0 & i\neq j\end{cases} \tag{15}$$

Substituting Eq. (12) into the linearized free-surface condition in Eq. (8), we obtain the linearized free-surface condition in the body-fixed coordinate system

$$\frac{\partial^2\phi_j}{\partial t^2}-2U_j\frac{\partial^2\phi_j}{\partial x_j\partial t}+U_j^2\frac{\partial^2\phi_j}{\partial x_j^2}+g\frac{\partial\phi_j}{\partial z_j}=0\,,\ \text{on } z = 0 \tag{16}$$

The boundary condition on the sea bottom and side walls, if any, can be expressed as:

$$\frac{\partial\phi_j}{\partial n}=0 \tag{17}$$

Besides, a radiation condition is imposed on the control surface to ensure that waves vanish at upstream infinity

$$\phi_j\to 0,\ \ \zeta_j\to 0\ \ as\ \sqrt{x_j^2+y_j^2}\to\infty \tag{18}$$

where ζ_j is the wave elevation as seen in the *j-th body-fixed* frame and is given by Eq. (30).

NUMERICAL SOLUTION

Eqs. (13) - (18) define a complete set of BVP. Each one of BVP is time-dependent but can be solved individually and independently; only a single speed of ship j appears in the free-surface condition in Eq.(16). The coupled problem is decoupled into N independent BVPs. At each time instant, the BVP in Eqs. (13) - (18) can be solved numerically. Following the work of Hess & Smith (1964), the boundaries are discretized into a number of quadrilateral panels with constant source density $\sigma(\boldsymbol{\xi_j})$, where $\boldsymbol{\xi_j} = (\xi_j, \eta_j, \varsigma_j)$ is a position vector on the boundaries in the *j-th body-fixed* frame and the free-surface (Bai & Yeung, 1974). Let $\mathbf{x_j} = (x_j, y_j, z_j)$ denote a point inside the fluid domain or on the boundary surface, the velocity potential ϕ can be expressed by a source distribution on the boundary of the fluid domain

$$\varphi(\mathbf{x_j})=\iint\limits_{S_f+S_c+\sum_{j=1}^{N}S_{bj}}\sigma(\boldsymbol{\xi}_\mathbf{j})G(\mathbf{x_j},\boldsymbol{\xi}_\mathbf{j})ds\,,\ j = 1, 2, \ldots, N \tag{19}$$

where $G=1/r$ is the Rankine-type source function, with r being the distance between $\boldsymbol{\xi}_\mathbf{j}$ and $\mathbf{x_j}$. More detailed numerical implementation on the solution of BVP can be found in Yuan et al. (2014b). The same in-house developed program MHydro is deployed in the present study as the framework to investigate ship hydrodynamics in restricted waterways. Special care should be taken to implement a suitable open boundary condition to satisfy Eq. (18). In numerical calculations, the computational domain is always truncated at a distance away from the ship hull. In general, waves will be reflected from the truncated boundaries and contaminate the flow in the computational domain. In the present study, a second-order upwind difference scheme is applied on the free-surface to obtain the time and spatial derivatives:

$$\frac{\partial^2 \phi_j}{\partial x^2}\left(\left(\mathbf{x_j}\right)_k\right)=\frac{1}{\Delta x^2}\left(\begin{array}{l}\frac{1}{4}\phi_j\left(\left(\mathbf{x_j}\right)_{k+4}\right)-2\phi_j\left(\left(\mathbf{x_j}\right)_{k+3}\right)\\+\frac{11}{2}\phi_j\left(\left(\mathbf{x_j}\right)_{k+2}\right)-6\phi_j\left(\left(\mathbf{x_j}\right)_{k+1}\right)\\+\frac{9}{4}\phi_j\left(\left(\mathbf{x_j}\right)_k\right)\end{array}\right) \tag{20}$$

Here k refers to the panel number. According to Bunnik (1999) and Kim et al. (2005), Eq. (18) can be satisfied consequently by applying Eq. (20). It should be noted that a second-order upwind difference scheme is applied at each body-fixed frame locally. This is essential to deal with ships travelling towards opposite directions.

For each individual velocity potential ϕ_j, the BVP is unsteady due to the time-dependent terms in Eq. (16). In previous studies on ship-to-ship interaction problem (Yeung, 1978; Yeung and Tan, 1980; Xu et al., 2016), within the framework of potential-flow theory, the BVP was not solved in time domain as the free-surface condition was assumed to be rigid. It was solved independently at each individual time step. The unsteady effect was only considered in the pressure calculations in Eq. (27). The unsteady interaction forces calculated in these studies are not exactly 'unsteady', since the velocity potential at each time step is not time dependent. The velocity potential obtained at t_n is not related to that obtained at t_{n-1}, and it will also not determine that at t_{n+1}. In the present study, the unsteady BVP will be solved in time domain by an iteration scheme. The essential steps are:

1. Determine the initial condition. We assume that at the initial stage of ship-to-ship operation, the moving ships are sufficiently far apart so that their interactions are negligible. Thus, the time dependent terms are removed from the free-surface condition in Eq. (16), and we have

$$U_j^2\frac{\partial^2\left(\phi_j^k\right)^*}{\partial x_j^2}+g\frac{\partial\left(\phi_j^k\right)^*}{\partial z_j}=0 \tag{21}$$

Here $(\phi_j^k)^*$ is the time-independent velocity potential at the time step k. The computational domain and the corresponding panel distribution at each time step k can be constructed and the steady BVP in Eqs. (13) to (15), (21), (17) and (18) can be solved straightforwardly by using the Rankine source panel method. The time-independent velocity potential $(\phi_j^k)^*$ can be obtained, which will be used as the initial guess to calculate the time derivatives of unsteady velocity potential ϕ_j^k in Eq. (22).

2. By applying the second-order backward difference scheme, the time derivatives in Eq. (16) can be calculated according to the following formulas

$$\begin{aligned}\frac{\partial\phi_j^k}{\partial t}&=\frac{1}{\Delta t}\left(\frac{3}{2}\left(\phi_j^k\right)^*-2\left(\phi_j^{k-1}\right)^*+\frac{1}{2}\left(\phi_j^{k-2}\right)^*\right)\\\frac{\partial^2\phi_j^k}{\partial t^2}&=\frac{1}{\Delta t^2}\left(\begin{array}{l}2\left(\phi_j^k\right)^*-5\left(\phi_j^{k-1}\right)^*+\\4\left(\phi_j^{k-2}\right)^*-\phi_j^*\left(\phi_j^{k-3}\right)^*\end{array}\right)\end{aligned} \tag{22}$$

3. Substituting Eq. (22) into Eq. (16), the following time-domain free-surface condition can be obtained

$$\frac{\partial^2\phi_j^k}{\partial t^2}-2U_j\frac{\partial\phi_j^k}{\partial t}\cdot\frac{\partial\phi_j^k}{\partial x_j}+U_j^2\frac{\partial^2\phi_j^k}{\partial x_j^2}+g\frac{\partial\phi_j^k}{\partial z_j}=0 \tag{23}$$

Solving the unsteady BVP in Eqs. (13) to (15), (23), (17) and (18), we can obtain the unsteady velocity potential ϕ_j^k. Residual errors of time derivatives of $\left|(\phi_j^k)^*-\phi_j^k\right|$ can be evaluated. If $\left|(\phi_j^k)^*-\phi_j^k\right|<\varepsilon$, the iteration stops and ϕ_j^k will be used to calculated the pressure and wave elevation. Otherwise, $(\phi_j^k)^*$ in Eq. (22) will be replaced by the newly obtained ϕ_j^k, and the iteration continues until $\left|(\phi_j^k)^*-\phi_j^k\right|<\varepsilon$. It is known that the iterative scheme has advantages of high accuracy and good numerical stability.

Once the unknown potential ϕ_j is solved on the plane $z = 0$ and on the body B_j, the unsteady pressure components under its individual coordinate system can be obtained from linearized Bernoulli's equation using numerical differentiation:

$$p_j\Big|_{\mathbf{x_j}}=-\rho\left[\frac{\partial\phi_j}{\partial t}\Big|_{\mathbf{x_j}}-U_j\frac{\partial\phi_j}{\partial x_j}\Big|_{\mathbf{x_j}}\right],\ j=1, 2, \ldots, N \tag{24}$$

We should point out that because of the first unsteady term in Eq. (24), the total pressure p in coordinate system $\mathbf{x_j}$ cannot be expressed directly as the sum of all the pressure components in their local

frames. To transfer the pressure from coordinate system $\mathbf{x_i}$ to $\mathbf{x_j}$, the following relation needs to be observed

$$\frac{d\phi_i}{dt}\Big|_{\mathbf{x_j}} = \left(\frac{\partial}{\partial t} - \left(U_j - U_i\right)\frac{\partial}{\partial x_i}\right)\phi_i\Big|_{\mathbf{x_j}}, \quad i, j = 1, 2, \ldots, N \tag{25}$$

It should be noted that the partial derivative symbol of the first term in Eq. (24) is retained to make it consistent with Eq. (12) where the potential is expressed in the body-fixed coordinate system $\mathbf{x_j}$. But here the body-fixed coordinate system $\mathbf{x_j}$ turns out to be in the reference frame for the other body-fixed coordinate system $\mathbf{x_i}$. Hence, $\partial\phi_j/\partial t$ is actually calculated as a total derivative by using Eq. (25). The unsteady pressure in coordinate system $\mathbf{x_i}$ ($i = 1, 2, \ldots, N, i \neq j$) can then be '*transferred*' to $\mathbf{x_j}$ as:

$$\begin{aligned} p_i\Big|_{\mathbf{x_j}} &= -\rho\left[\left(\frac{\partial}{\partial t} - \left(U_j - U_i\right)\frac{\partial}{\partial x_i}\right)\phi_i\Big|_{\mathbf{x_j}} - U_i\frac{\partial\phi_i}{\partial x_i}\Big|_{\mathbf{x_j}}\right] \\ &= -\rho\left(\frac{\partial}{\partial t} - U_j\frac{\partial}{\partial x_i}\right)\phi_i\Big|_{\mathbf{x_j}}, \quad i, j = 1, 2, \ldots, N \end{aligned} \tag{26}$$

Note the subtle differences between Eq. (24) and (26). The total pressure p in coordinate system $\mathbf{x_j}$ can be written as

$$p\Big|_{\mathbf{x_j}} = \sum_{i=1}^{N} p_i\Big|_{\mathbf{x_j}} = -\rho\sum_{i=1}^{N}\left(\frac{\partial}{\partial t} - U_j\frac{\partial}{\partial x_i}\right)\phi_i\Big|_{\mathbf{x_j}}, \; i, j = 1, 2, \ldots, N \tag{27}$$

Integrating the pressure over the hull surface, we can express the forces (or moments) on the i-th hull induced by the j-th ship as:

$$F_k^j = \iint_{S_j} p n_k dS, \; j = 1, 2, \ldots, N \tag{28}$$

where k = 1, 2, …, 6, representing the force in surge, sway, heave, roll, pitch and yaw directions, and

$$n_k = \begin{cases} \mathbf{n}, & k = 1, 2, 3 \\ \mathbf{x} \times \mathbf{n}, & k = 4, 5, 6 \end{cases} \tag{29}$$

The free-surface elevation can be obtained from dynamic free-surface boundary condition in Eq. (7). Similar to the pressure expression, the unsteady wave elevation in coordinate system $\mathbf{x_i}$ ($i = 1, 2, \ldots, N, i \neq j$) can be transferred to $\mathbf{x_j}$ as:

$$\zeta_i\Big|_{\mathbf{x_j}} = -\frac{1}{g}\left(\frac{\partial}{\partial t} - U_j\frac{\partial}{\partial x_i}\right)\phi_i\Big|_{\mathbf{x_j}}, \; i, j = 1, 2, \ldots, N \tag{30}$$

The *total* wave elevation in coordinate system $\mathbf{x_j}$ can be written as

$$\zeta\Big|_{\mathbf{x_j}} = -\frac{1}{g}\sum_{i=1}^{N}\left(\frac{\partial}{\partial t} - U_j\frac{\partial}{\partial x_i}\right)\phi_i\Big|_{\mathbf{x_j}}, \; i, j = 1, 2, \ldots, N \tag{31}$$

We note that we have not imposed a Kutta condition at the stern, as a first approximation, or equivalently, the stern is pointed.

VALIDATIONS OF NUMERICAL MODEL

The convergence study is carried out on two identical Wigley III hulls in head-on encounter. We calculate the lateral force and wave elevation to exam the convergence of the superposition method with different time steps (Δt). The panel size to ship length ratio at each Froude number is fixed at $\Delta x/L = 1/\kappa$. The time then can be non-dimensionalized by

$$t' = \Delta x / U = \frac{1}{\kappa F_n}\sqrt{\frac{L}{g}} \tag{32}$$

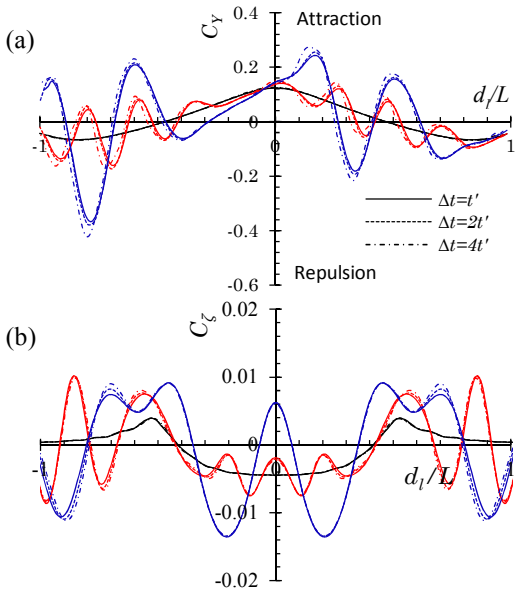

Figure 3: Convergence study on two identical Wigley III hulls (Journee, 1992) in head-on encounter with d_t/B=2, d_t being the lateral separation between two ships (a) Sway force; (b) wave profile at the center line between two ships at the moment of side-by-side

configuration (d_l=0). The black, red and blue cures correspond to F_n=0.1, 0.2 and 0.3 respectively. C_Y and C_ζ is non-dimensionalized by $\frac{1}{2}\rho BT|U_1U_2|$ and by $2\pi|U_1U_2|/g$ respectively.

In the present study, κ=60 was found adequate to obtain a convergent result. The results shown above in **Figure 3** confirm the convergence of the present superposition method by reducing the time-stepping. It should be noted that the convergence becomes slower as the encounter speed increases.

Model-test data on ship-to-ship interaction with different speeds as a parameter is rather rare. To run the tests, an auxiliary carriage must be installed, in addition to the main tow carriage. Therefore, the encountering tests were not included in Oltmann (1970). In the present study, as another check, the benchmark data published by Vantorre, et al. (2002) is used to validate the numerical results of encountering cases. Two ship models with scale factor 1/75 are used for encountering or overtaking tests (referred as Model D and Model E). The main particulars of Model D (j=2) and Model E (j=1) in model scale can be found in Table 1. In the model test, Model E was towed by the main carriage along the center line (y = 0) of the tank, while Model D was towed by an auxiliary carriage. The transverse separation is $dt = B_D + 0.5B_E$ and the water depth d is $0.248m$.

Table 1: Main particulars of Model D and Model E in Vantorre et al (2002).

	Model E (j=1)	Model D (j=2)
Length *(m)*	L_E = 3.824	L_D = 3.864
Breadth *(m)*	B_E = 0.624	B_D = 0.55
Draft *(m)*	T_E = 0.207	T_D = 0.18
Block coefficient	C_{BE} = 0.816	C_{BD} = 0.588

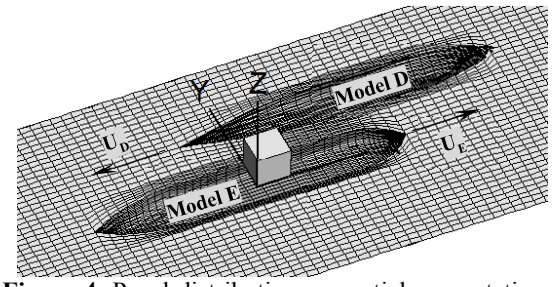

Figure 4: Panel distribution on partial computational domain. There are 9,950 panels distributed on the entire computational domain: 1,900 on the wetted body surface of Model E, and 2,170 on the wetted body surface of Model D, 5,880 on the free-surface. The free-surface is truncated at $2L_E$ upstream and $2L_E$ downstream with regard to the body-fixed frame on Model E.

Figure 4 shows the mesh distribution on the partial computational domain when Model E encounters Model D. It should be noted that the side walls of the tank are not modeled. In order to reduce the panel number, the free surface is truncated at $0.27L_E$ and $0.42L_E$ laterally with regard to Model D and Model E respectively. In calm water test, it has been proved by Yuan and Incecik (2016b) that the side wall effects are negligible at d_{sb} / L > 0.25 and F_n < 0.25. It should also be noted that in the encountering simulation, the longitudinal separation d_l is measured in body-fixed frame on Model E. The longitudinal separation between two ships at the moment shown in **Figure 4** has a positive sign. The time step Δt in the numerical calculation is $0.18s$. The numerical results, as well as the experimental measurements, are shown in **Figure 5**.

Figure 5 shows the interaction forces on Model E at F_n=0.039 encountered by Model D at F_n=0.078. These two case studies aim to validate the feasibility of the present superposition method in simulating the ships moving in opposite directions. In this validation case, the forces on both ships are calculated numerically. However, only the forces on Model E, which was towed by the main carriage, were measured in model tests. Generally, the agreement between present potential-flow solver (MHydro) and experimental measurement is very good. It indicates the potential flow method is applicable for predicting the hydrodynamic interactions between two ships with different speeds.

It is observed from **Figure 5**a that the resistance (F_1) is overestimated by the present potential-flow solver, even though the viscous effect is not taken into account. It indicates the hydrodynamic interaction force plays a dominant role in total resistance, and the frictional component due to the viscosity is negligible. The negative values shown in **Figure 5**a represent the resistance that is opposite to the moving direction, while the positive values represent a thrust which is the same as the moving direction. An interesting finding is that a very large thrust force is observed at d_l / L_E = -0.5 during the encountering maneuvering. Physically it can be explained that before encountering ($0 < d_l / L_E < 1$), the presence of the other moving vessel stops the water from spreading evenly into the surrounding field. As a result, the pressure distributed over ship bow increases. At the same time, the pressure distributed over ship stern retains the same level. An increased resistance is expected by pressure integral. After encountering ($-1 < d_l / L_E < 0$), the high pressure area transfers to the ship stern, which will correspondingly lead to a propulsive force.

During the encountering process, the symmetry of the flow with respect to the starboard and the port

side is violated by the presence of the other vessel. The maximum asymmetric flow is observed when the midships of the two ships are aligned ($d_l / L_E \approx 0$), and the suction force reaches its peak value (see **Figure 5**b). The pressure distribution is not only asymmetric with respect to port and starboard, but also with respect to the bow and the stern. Consequently, a yaw moment will be induced, as shown in **Figure 5**c. Generally, there are four peaks of yaw moment during passing and encountering maneuvering, which appear at $d_l / L_E \approx -0.6$, $d_l / L_E \approx -0.1$, $d_l / L_E \approx 0.4$ and $d_l / L_E \approx 0.9$. Based on these peaks, some empirical formulas were established to model the interaction moment (Vantorre et al., 2002; Varyani et al., 2002; Lataire et al., 2012). However, as the number of the peaks is not predictable, the applicability of such empirical formulas is limited. It should be noted that in ship-bank and ship-lock problem, the potential flow method fails to predict the sign of the yaw moment because of the weak lifting force caused by cross-flow effects at the stern

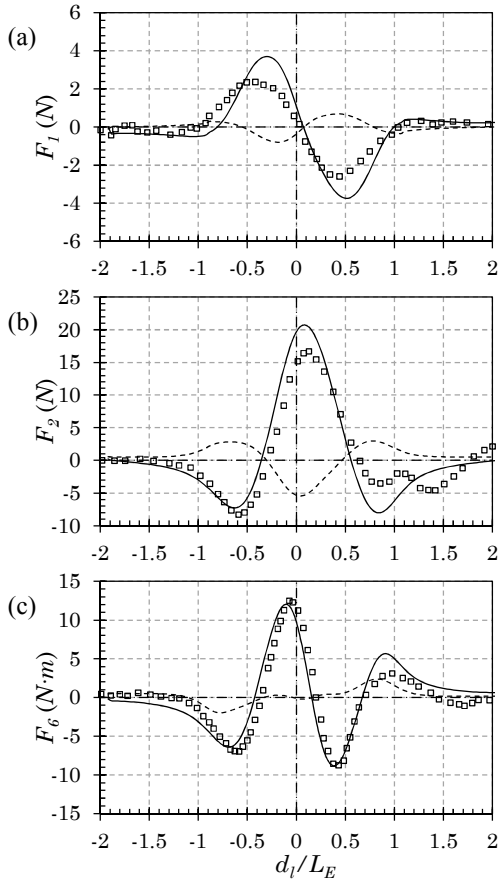

Figure 5: (a) The resistance, (b) the sway force and (c) the yaw moment on Model E (j=1) at F_n=0.039 encountered by Model D (j=2) at F_n =0.078. The positive d_l values denote that Model D is in the upstream side of Model E. As Model D moves to the downstream side, d_l becomes negative. EFD results are published by Vantorre et al. (2002).

(Yuan, Yu, and Incecik, 2016a). However, in ship-to-ship problem, the hydrodynamic interaction is much more important than the cross-flow effects

DISCUSSIONS ON FREE-SURFACE EFFECTS

The predictions of the yaw moment by a potential-flow solver are therefore reliable. After the aforementioned validations against physical model tests, the present superposition method was extended to investigate the free-surface effects. Here, we study the interactions between two identical Wigley III hulls in head-on encounter. The geometry of the hull can be found in Journee (1992).

Figure 6 shows the panels distributed on the partial computational domain. The panel number per ship length κ=60. $\Delta t=2t'$ is applied in all of the numerical simulations reported below. We computed the interaction forces in 6DoF (6 Degrees of Freedom), as well as the total wave elevation.

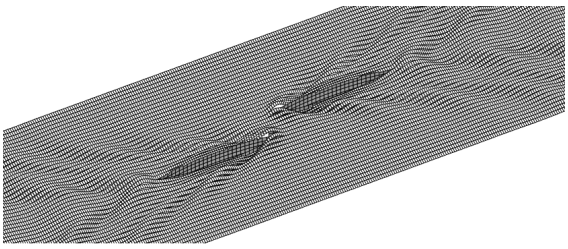

Figure 6: Panel distribution on the computational domain of two identical Wigley III hulls in head-on encounter with F_n=0.3, d_l/B=2, and d_l/L=1. There are 17,760 panels distributed on the entire computational domain: 600 on the wetted body surface of each hull and 16,560 on the free-surface. The computational domain is truncated at 2L upstream, 2L downstream and 0.5L laterally with regard to the body-fixed reference frame.

Figure 7 shows the results of the lateral (sway) forces on two identical Wigley III hulls in head-on encounter with d_l/B=2. Here we compare the results obtained by using three different methods. In the first method, the encountering problem is treated as a "steady problem," with the steady linearized free-surface condition applied. Mathematically, in the pressure calculation, the first term in Eq. (27) is not used. Meanwhile, the first two time-dependent terms in Eq. (16) are also not taken into account. It has been found to be an efficient method to deal with the

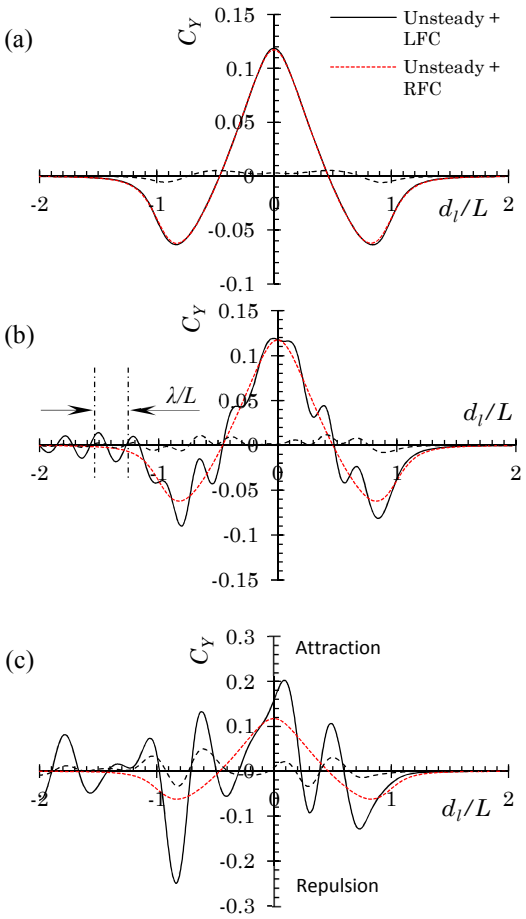

Figure 7: Sway force acting on two identical Wigley III hulls in head-on encounter with d_l/B=2. (a) F_n=0.1; (b) F_n=0.2; (c) F_n=0.3. d_l/L=0 corresponds to the moment $t=t_s$, when the midships of the two ships are aligned. $d_l/L>0$ corresponds to $t<t_s$, $d_l/L<0$ corresponds to $t>t_s$. C_Y is non-dimensionalized by $\frac{1}{2}\rho BT|U_1U_2|$. LFC indicates that the linearized free-surface condition is used; RFC indicates that the rigid-wall free-surface condition is used.

steady-state type problems, e.g., interactions between two ships travelling with the same speed (Yuan et al., 2015), or between the hulls of a catamaran or trimaran (Shahjada Tarafder and Suzuki, 2007). In the second method, the encountering is treated as a full unsteady problem, while the rigid condition is applied on the free surface. Mathematically, the free-surface condition in Eq. (16) is replaced by an impermeable boundary condition. The BVP therefore is solved as a steady problem with no memory effects. The only unsteady effects are reflected by the time-derivative term in Eq. (27). Nearly all the published studies on the ship-to-ship problem are based on this partially unsteady (Yeung, 1978; Korsmeyer et al., 1993; Zhou et al., 2012; Xu et al., 2016). The advantage of this rigid-free-surface method is obvious. As an imaging technique can be applied on the free surface, it does not require panels to be distributed on the free surface. It significantly reduces the panel number, herein reducing the calculation time to solve the BVP. However, this method is only applicable when the speed of the ships is low. The third method proposed by the present study takes all the unsteady effects into account. The time derivatives in both Eq. (16) and Eq. (27) are considered. The BVP is solved in the time domain by using an iteration scheme. The advantage of this fully unsteady method is that it can predict the hydrodynamic interaction induced by the ship-generated waves. But the panels must be distributed on the free-surface, which not only increases the total mesh number, but only add difficulties to construct the computational domain at each time step. To deal with this issue, we developed a dynamic meshing technique to generate the mesh automatically at each time step. With regard to the computational time, the third method takes longer than the other two methods. But within the framework of potential-flow theory, the computational time is still very satisfactory. Most of the computational efforts are spent on generating the so-called coefficient matrix (Hess and Smith, 1964) Even though it involves time iteration, the coefficient matrix retains unchanged. The time scale to solve the unsteady BVP for each time step is few minutes.

The results shown in **Figure 7** clearly demonstrate the effects of unsteady pressure and unsteady free surface. Here, we note that the unsteady pressure term in Eq. (27) is very important at all the range of encountering speeds, while the free-surface effect is only important when the encounter speed is moderate or high. Ignoring the unsteady pressure term in Eq. (27) will lead to mis-estimation of the interaction force. At F_n = 0.1, the free-surface elevation and hydrodynamic interaction are mainly determined by the near-field (non-wave-like) disturbances. The rigid free-surface condition (RFC) is adequate to predict the interaction forces, as shown in **Figure 7**a. As the Froude number increases to F_n =0.2, the far-field waves become manifest, and the interaction force oscillates correspondingly, as shown in **Figure 7**b. However, at F_n =0.2, the interaction is still dominated by the near-field disturbance. The contribution of the force induced by far-field waves is smaller than that induced by the near-field disturbance. The fluctuations due to the far-field waves will not deviate from the near-field induced forces. The interaction force predicted by rigid free-surface condition is symmetric with respect to d_l/L=0.

But this symmetry property is altered by the presence of the far-field waves. As the far-field waves could not propagate ahead of the ship, the free-surface effect cannot be observed before the encountering taken place (d_l/L>1). As the encountering ships are maneuvering to each other's wake region, the free-surface effect can then be observed, and some wave-induced fluctuations can be observed at d_l/L<1 correspondingly. These fluctuations will not disappear (but the amplitude will decrease) after the encountering operation. The relationship between the near- and far-field induced force is very similar to that between low- and wave-frequency surge or sway motions of a floating structure in irregular waves (Yuan et al., 2014a). The free-surface effect becomes even more significant at F_n = 0.3. The force amplitude induced by the far-field waves is larger than that induced by the near-field disturbance, as shown in **Figure 7**c. There are only three peaks induced by near-field disturbance. However, the peaks altered by the far-field waves are unpredictable. Therefore, the empirical formulae based on low speed model (Vantorre et al., 2002; Varyani et al., 2002; Lataire et al., 2012) are not applicable to predict the interaction forces when the wave effects become important. It can be concluded that the free-surface effects must be taken into account at F_n > 0.2.

Figure 8 and **Figure 9** show the effect of encountering speed and lateral separation on the interaction forces in 6 DoF. When the lateral clearance between two ships is small (d_l/B=2), both near-field and far-field disturbance can be observed. However, only the far-field wave disturbance can be observed at high speed encountering when the lateral clearance becomes large (d_l/B=10). In a practical maneuvering operation, a large lateral clearance encountering is more likely to occur. Due to the free-surface waves, the unsteady interactive forces will affect the maneuverability of a ship in the confined waterways.

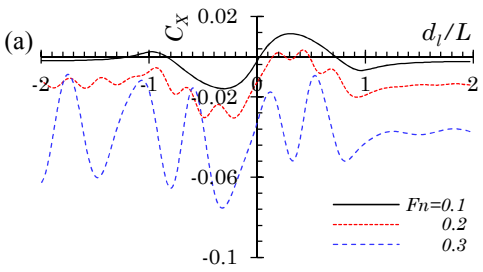

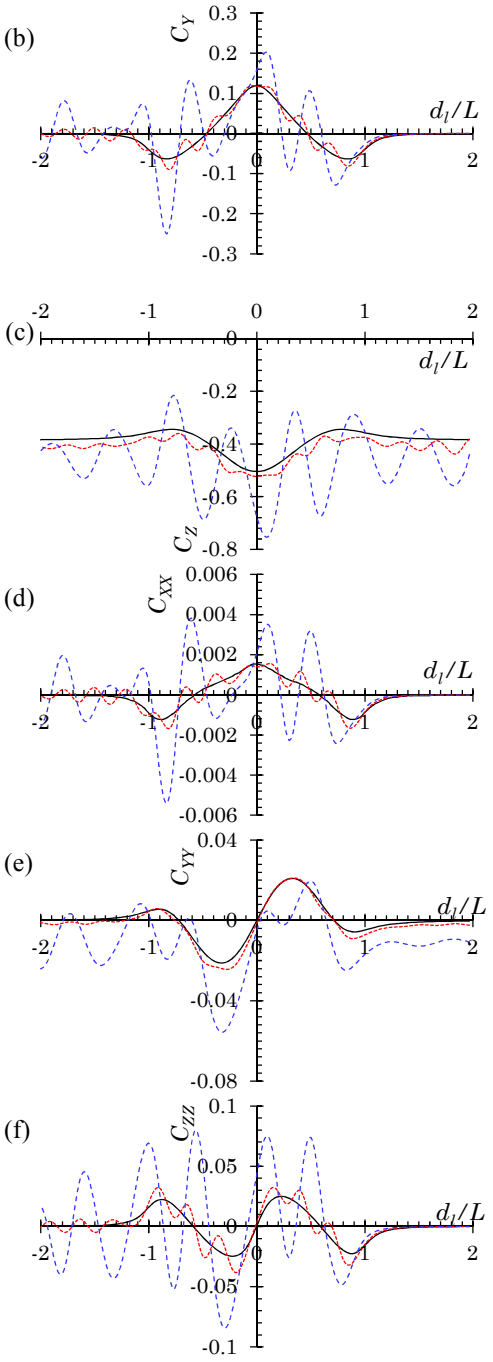

Figure 8: Forces and moments acting on two identical Wigley III hulls in head-on encounter with d_l/B=2. (a) Surge force; (b) sway force; (c) heave force; (d) roll moment; (e) pitch moment; (f) yaw moment. Forces are non-dimensionalized by $\frac{1}{2}\rho BT|U_1U_2|$ and moments are non-dimensionalized by $\frac{1}{2}\rho BTL|U_1U_2|$.

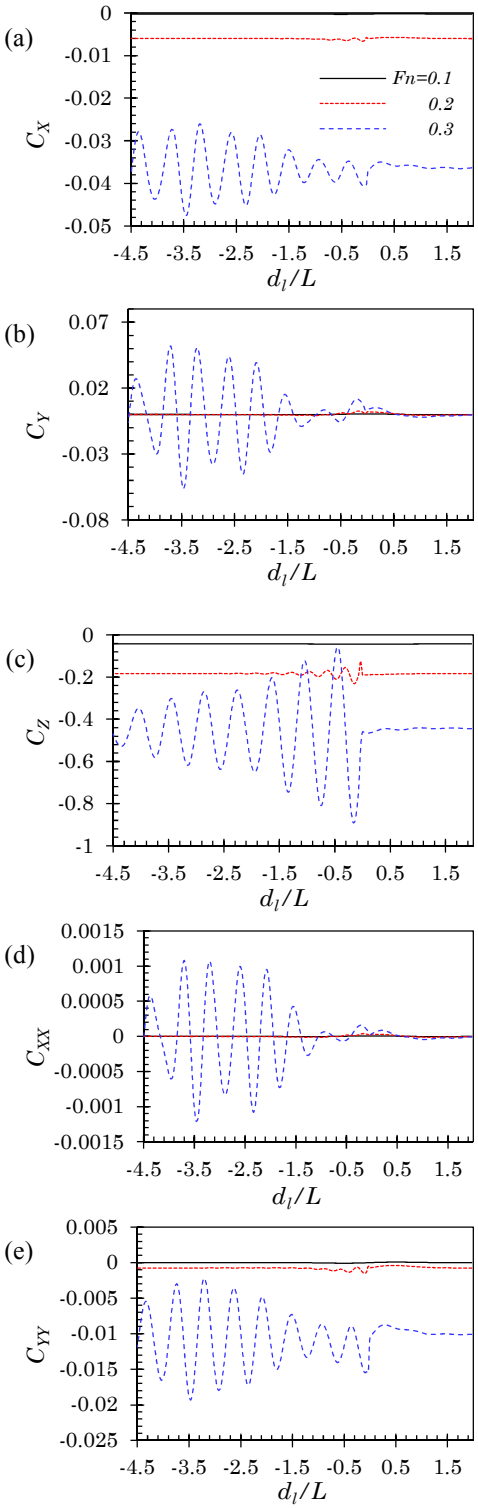

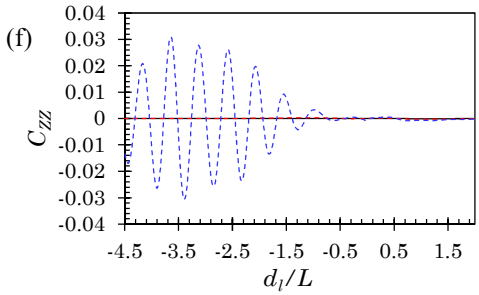

Figure 9: Forces and moments acting on two identical Wigley III hulls in head-on encounter with d_l/B=10. (a) Surge force; (b) sway force; (c) heave force; (d) roll moment; (e) pitch moment; (f) yaw moment.

Figure 10 shows the wave profile at the moment when the midships of two Wigley hulls are aligned. The 'Steady' indicates the first two terms in Eq. (16) are ignored, while 'Unsteady' indicates the BVP is solved fully in the time domain by using an iteration scheme. At low Froude number F_n=0.1, the unsteady effect on free-surface condition is not essential. As the wave elevation is dominant by the near-field disturbance, the wave-like fluctuations can hardly be observed at low forward speed. At moderate Froude number, the unsteady effect becomes manifest, especially at the gap between two aligned ships (-0.5<x/L>0.5). as the Froude number increases to F_n=0.3, the difference between 'Steady' and 'Unsteady' can be observed in a wider range of x/L, especially at the bow (x/L=0.5) and stern (x/L=-0.5) areas. **Figure 11** shows the wave elevation components obtained by the present superposition principle. It should be noted that the total wave elevation presented in **Figure 11**c is not the simple superposition of the waves produced by two individual hulls moving towards opposite direction. When we calculate the wave elevation produced by B_1, the presence of B_2 is also considered, treated as an obstacle, by being momentarily stationary in the body-fixed frame of B_1. Therefore, the diffraction and reflection by B_2 is considered in the present study. These reflected waves can be seen clearly from **Figure 11**a and b.

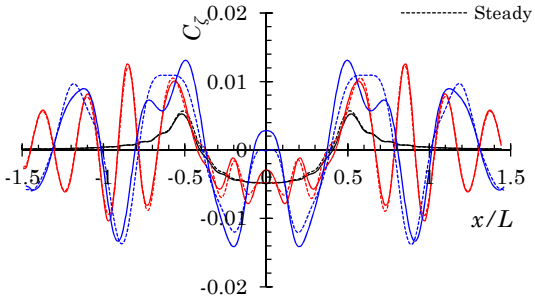

Figure 10: Wave profiles at the center line between two identical Wigley III hulls in head-on encounter with d_l/B=2, d_l/L =0 and F_n=0.3. The black, red and blue curves correspond to F_n=0.1, 0.2 and 0.3 respectively.

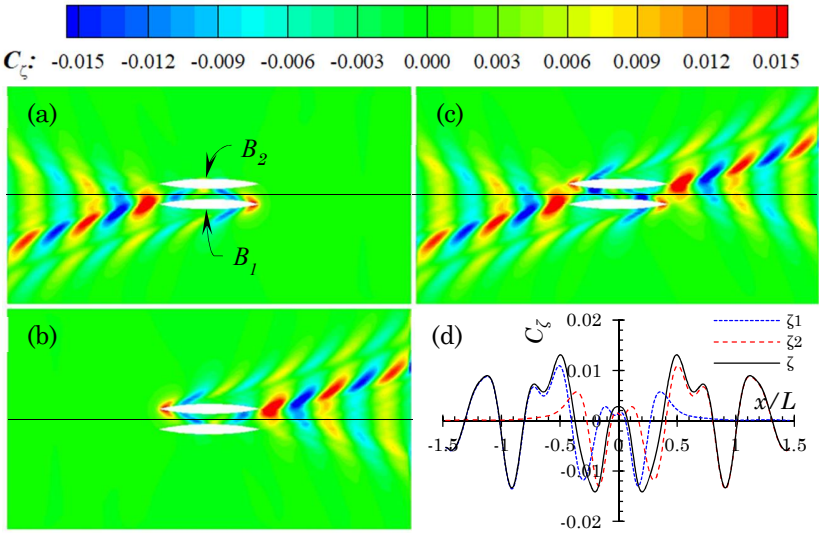

Figure 11: Waves produced by two Wigley III hulls in head-on encounter with d_l/B=2, d_l=0 and F_n=0.3. (a) $C_{\zeta 1}$, the waves produced by B_1 moving at F_n=0.3 while B_2 is momentarily stationary in the body-fixed frame of B_1; (b) $C_{\zeta 2}$, the waves produced by B_2 moving at U_2 while B_1 is momentarily stationary in the body-fixed frame of B_2; (c) C_ζ, the total waves superposing $C_{\zeta 1}$ and $C_{\zeta 2}$; (d) Wave profile at the centre line between two hulls shown in (a), (b) and (c). x in the abscissa of (d) refers to the midship-to-midship distance between the left-moving ship and the encountered ship.

CONCLUSIONS

A linearized free-surface boundary condition was used to solve the BVP involved in multiple bodies travelling with various speeds. Based on superposition principal, the traditional coupled BVP could be decoupled into N (assuming there are N bodies) sets of independent unsteady BVPs, which can be solved individually in the ime domain. The advantage of this decoupled method is that the free-surface boundary condition can be taken into consideration for each set of the independent BVPs. Thus, the unsteady hydrodynamic interaction problem can be solved in a fully unsteady manner, and the far-field wave effect can be accounted for fully.

The present formulation provides an effective way to predict the free-surface effects, with particular application for calculating the lateral interaction force on arbitrary number of ships, each with its own speed. By integrating the present superposition method into a Rankine source (simple-source) panel code, we calculated the unsteady hydrodynamic interaction forces and wave elevation when two ships were under passing, overtaking and encountering operations. Experimental measurements confirm the applicability of the present approach. Numerical results indicate the near-field disturbances are the most important component of the interaction force when the encountering speed is low. As the encountering speed increases, the interaction force induced by the far-field waves becomes manifest gradually. It was found the free-surface effects must be considered at $F_n > 0.2$ for slender ships. For blunt-body ships, the lower limit of Froude number is smaller. When the encountering speed reaches $F_n = 0.3$, the free-surface effect becomes the dominant component. The interaction force induced by the divergent waves could reach a very large value, which may cause ship accidents, such as grounding, capsizing or collisions. By increasing the separation distance between encountering ships could

reduce the interaction amplitude, but not significantly. At high encountering speed, the free-surface must be taken into account even though the lateral separation between ships is large.

The superposition method proposed in the present study is not limited to solving the unsteady interaction problem between ships. It can also be applied to predict the hydrodynamic interactions between competitive swimmers in a swimming pool, or between aquatic animals swimming near the free surface. The present approach provides a rational and rapid (real-time level) tool for analyzing and computing interaction effects, without going through a lengthy detailed CFD type computations, which would be prohibitively slow (e.g., Zou and Larsson (2013a)) and have yet reached a state to effectively model unsteady multi-body interaction.

ACKNOWLEDGEMENTS

The first author acknowledges the financially support by a Sir David Anderson Award for his visit to UC Berkeley during which this work was formulated. The second author acknowledges partial support of the American Bureau of Shipping via an endowed chair in Ocean Engineering at UC Berkeley. Discussions with Dr. Lu Wang and Mr. Dongchi Yu of UC Berkeley during the course of this work are appreciated.

REFERENCES

Bai, K.J., Yeung, R.W., "Numerical solutions to free-surface flow problems," Proceedings of the 10th Symposium on Naval Hydrodynamics, 1974, 609-646, Cambridge, Massachusetts, USA.

Bunnik, T., "Seakeeping calculations for ships, taking into account the non-linear steady waves," PhD thesis, 1999, Delft University of Technology, The Netherlands.

Collatz, G., "Potentialtheoretische Untersuchung der hydrodynamischen Wechselwirkung zweier Schiffskörper." Jahrbuch der Schiffbautechnischen Gesellschaft, 1963, **57**, 281-389.

Dand, I.,. "Some aspects of tug-ship interaction," Proceedings of the 4th Int. Tug Convention, New Orleans, October 20-23, 1975

Fonfach, J. M. A., Sutulo, S., & Guedes Soares, C. "Numerical study of ship-to-ship interaction forces on the basis of various flow models," Proceedings of the 2nd International Conference on Ship Maneuvering in Shallow and Confined Water, 2011, pp. 18-20, Trondheim, Norway,

Hess, J.L., Smith, A.M.O., "Calculation of nonlifting potential flow about arbitrary three-dimensional bodies." Journal of Ship Research, 1964, **8** (2), 22-44.

Jin, Y., Chai, S., Duffy, J., Chin, C., Bose, N., Templeton, C., "RANS prediction of FLNG-LNG hydrodynamic interactions in steady current," Applied Ocean Research, 2016, **60**, 141-154.

Journee, J.M.J., "Experiments and calculations on 4 Wigley hull forms in head waves," Report No. 0909. Ship Hydromechanics Laboratory, Delft University of Technology, 1992, The Netherlands.

Kijima, K., Yasukawa, H., "Manoeuverability of ships in narrow waterway," Journal of the Society of Naval Architects of Japan, 1985. **23,** 25-37.

Kim, Y., Yue, D.K.P., Connell, B.S.H., "Numerical dispersion and damping on steady waves with forward speed," Applied Ocean Research, 2005, **27** (2), 107-125.

Korsmeyer, F.T., Lee, C.-H., Newman, J., N., "Computation of ship interaction Forces in Restricted Waters," Journal of Ship Research, 1993, **7** (4), 298-306.

Lataire, E., Vantorre, M., Delefortrie, G., Candries, M., "Mathematical modelling of forces acting on ships during lightering operations," Ocean Engineering , 2012 **55,** 101-115.

Meng, Q. and Wan, D., "URANS Studies of Ship-to-Ship Interactions during Lightering Operations," Proceedings of the 31st Symposium on Naval Hydrodynamics, 11-16 September, 2016. Monterey, California.

Oltmann, V.P., "Experimentelle Untersuchung der hydrodynamischen Wechselwirkung schiffsähnlicher Körper, Schiff und Hafen, 1970, **22**, 701-707.

Pinkster, J.A., The influence of a free surface on passing ship effects. International Shipbuilding Progress, 2004. **51** (4), 313-338.

Pinkster, J. A., & Bhawsinka, K., "A real-time simulation technique for ship-ship and ship-port interactions." Proceedings of the 28th International Workshop on Water Waves and Floating Bodies (IWWWFB 2013), 2013, L'Isle sur la Sorgue, France.

Shahjada Tarafder, M., Suzuki, K., "Computation of wave-making resistance of a catamaran in deep water using a potential-based panel method", Ocean Engineering, 2007, **34** (13), 1892-1900.

Sian, A.Y., Maimun, A., Ahmed, Y., "Simultaneous ship-to-ship interaction and bank effect on a vessel in restricted water," Proceeding of the 4th MASHCON, 2016. Hamburg, Germany.

Söding, H., Conrad, F., "Analysis of overtaking manoeuvres in a narrow waterway," Ship Technology Research, 2005. **52**, 189-193.

Tuck, E.O., "Shallow water flows past slender bodies," Journal of Fluid Mechanics, 1966, 26, 81–95.

Tuck, E.O., Newman, J.N., "Hydrodynamic interactions between ships," Proceedings of 10th Symposium on Naval Hydrodynamics, 1974, 35-70, Cambridge, Massachusetts, USA,

Vantorre, M., Verzhbitskaya, E., Laforce, E.,. "Model test based formulations of ship–ship interaction forces," Ship Technology Research, 2002, **49**, 124-141.

Varyani, K.S., McGregor, R., Wold, P., "Interactive forces and moments between several ships meeting in conÞned waters," Control Engineering Practice, 1998, **6,** 635-642.

Varyani, K.S., McGregor, R., Wold, P.,. "Identification of trends in extremes of sway–yaw interference for several ships meeting in restricted waters," Ship Technology Research, 2002, **49,** 174-191.

Xiang, X., Faltinsen, O.M., "Maneuvering of Two Interacting Ships in Calm Water," 11th International Symposium on Practical Design of Ships and Other Floating Structures, 2010, Rio de Janeiro, RJ, Brazil.

Xu, H., Zou, Z., Zou, L., Liu, X., "Unsteady hydrodynamic interaction between two cylindroids in shallow water based on high-order panel method," Engineering Analysis with Boundary Elements, 2016. **70**, 134-146.

Yeung, R.W., "Surface Waves due to a Maneuvering Air-Cushion Vehicle," Journal of Ship Research, 1975, 19 (4), 581-607.

Yeung, R.W., "On the interactions of slender ships in shallow water," Journal of Fluid Mechanics, 1978, **85,** 143-159.

Yeung, R.W., Tan, W.T., "Hydrodynamic interactions of ships with fixed obstacles," Journal of Ship Research, 1980, **24** (1), 50-59.

Yuan, Z.-M., Incecik, A., Ji, C., "Numerical study on a hybrid mooring system with clump weights and buoys," Ocean Engineering, 2014a, **88** (1), 1-11.

Yuan, Z.-M., Incecik, A., Jia, L., "A new radiation condition for ships travelling with very low forward speed," Ocean Engineering, 2014b, **88**, 298-309.

Yuan, Z.M., He, S., Paula, K., Incecik, A., Turan, O., Boulougouris, E., "Ship-to-Ship Interaction during Overtaking Operation in Shallow Water," 2015, .Journal of Ship Research, **59** (3), 172-187.

Yuan, Z.M., Incecik, A., "Investigation of ship-bank, ship-bottom and ship-ship interactions by using potential flow method," Proceedings of 4th International Conference on Ship Manoeuvring in Shallow and Confined Water, 2016a., Hamburg, Germany.

Yuan, Z.M., Incecik, A., "Investigation of side wall and ship model interaction," Int Conference on Marinte Technology (ICMT2016), 2016b, Harbin, China.

Zhou, X., Sutulo, S., Guedes Soares, C., "Computation of ship hydrodynamic interaction forces in restricted waters using potential theory," Journal of Marine Science and Application, 2012, **11** (3), 265-275.

Zou, L., Larsson, L., "Computational fluid dynamics (CFD) prediction of bank effects including verification and validation," Journal of Marine Science and Technology, 2013a, **18** (3), 310-323.

Zou, L., Larsson, L., "Numerical predictions of ship-to-ship interaction in shallow water," Ocean Engineering, 2013b **, 7**, 386-402.